Interdependencies between the distribution of density, land use, and the cost-effectiveness of district cooling systems

Working Paper

Author(s):
Shi, Zhongming; Fonseca, Jimeno A.; Schlueter, Arno

Publication date:
2020

Permanent link:
https://doi.org/10.3929/ethz-b-000391819

Interdependencies between the distribution of density, land use, and the cost-effectiveness of district cooling systems

Zhongming Shi [a, b, *], Jimeno A. Fonseca [a,b], Arno Schlueter [a,b]

[a] Future Cities Laboratory, Singapore-ETH Centre, 1 Create Way, CREATE Tower, Singapore 138602, Singapore
[b] Architecture and Building Systems, ETH Zurich, Stefano-Franscini-Platz 1, Zurich 8093, Switzerland

Abstract
Density and land use are two fundamental components controlled in a city's master plan. Together, they affect spatial and temporal distributions of the cooling demand of tropical high-density cities. This work studied how the design of density and land use impacts the cost-effectiveness of district cooling systems. To approach this, we took the street layout plan of Downtown Singapore and generated hundreds of designs of density and land use using Grasshopper and the quasi-Monte Carlo Saltelli sampler. Five independent input variables were used for sampling. They feature the spatial distribution of floor area ratio and three land use types including residential, office, and retail. We assessed the cost-effectiveness for the district cooling systems in each sample with a simulation program called the City Energy Analyst. To determine the effects of various designs on the cost-effectiveness of the district cooling systems, we performed the Sobol' sensitivity analysis. We found that the Global land use ratios and the spatial distributions of density have the dominant role, while the spatial distributions of land use have a minor influence on the cost-effectiveness of district cooling systems. Urban planners and designers may use the result of this study in the design of density and land use in a district of high-density cities serviced by district cooling systems.

Keywords: density; land use; district cooling systems; capital expenditure; operational expenditure; energy-driven urban design

1. Introduction

Floor area density and land use assignment are of great importance in the field of urban design. In the master plan of many cities, their corresponding metrics are often witnessed in the form of floor area ratio and land use ratios for a mixed-use development. The example master plan in Figure 1 presents the control of floor area ratio in numbers and land use in colors (Urban Redevelopment Authority, 2014). At the building level, they constrain the architectural design by restricting the quantity of gross floor area for each land use type. For example, for two sites of the same high floor area ratio, the more residential-dominated site may tend to have much slimmer building volume design for the purposes of natural sunlight accessibility. At a larger scale of district or city, floor area density and land use assignment together spatially shape the morphological cityscape and, more importantly, temporally affect the flow of human and all forms of traffic along the street or the piping network. For example, the locations of job and home create the flows of commuters; the utility consumers with various needs and schedules affect the distribution of utilities.

Figure 1. Density and land use control in an exemplary master plan (Urban Redevelopment Authority, 2014).

In tropical high-density cities, district cooling systems (DCS) which rely on a centralized cooling production are efficient means of cooling energy supply (UNEP, 2015). As shown in Figure 2, the basic components of a DCS include district cooling plant(s), pumps, and piping networks. The latter two comprising the distribution network of a DCS help circulate the chilled water between the district cooling plant and the end-users. The DCS cost-effectiveness is associated with both the DCS capital and operational expenditures. The former is determined by the sizing of each DCS component and its pricings. Besides that spent to fulfill the district's cooling demand, the latter also includes that spent on the thermal loss and pressure drop in the distribution network. The peak thermal loss in the DCS distribution, though much lower than that in the district heating system, can surpass as much as 10% of the cooling supply (Li et al., 2017; McCabe et al., 1995), while the pressure drop may contribute up to 10% of the total DCS electricity consumption (Guelpa et al., 2016; Li et al., 2017).

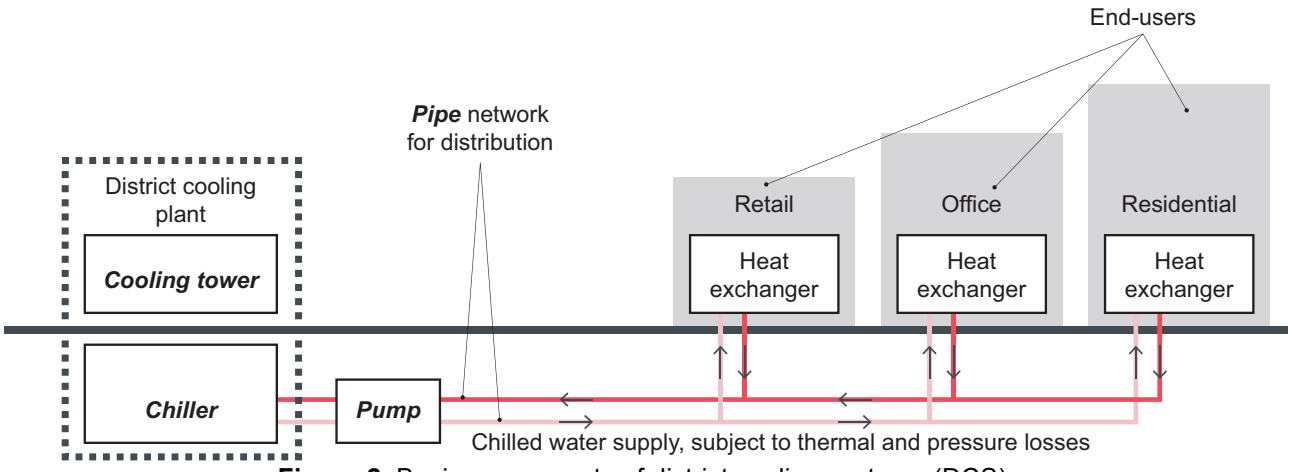

Figure 2. Basic components of district cooling systems (DCS).

The impacts on the DCS cost-effectiveness by the distribution of floor area density and land use can be explained in the following aspects. First, the sizing of each DCS component is based on its annual peak cooling demand to accommodate. Spatially, the floor area density influences the building volumes which affects the solar radiation received on the building surfaces and the (peak) cooling demand (Cheng et al., 2006). Temporally, the combination of various land use types influences a district's fluctuating cooling demand throughout each hour of the day and, thus, affects the DCS design as well as its cost-effectiveness.

Second, in the pipes of chilled water distribution, the pressure drop is influenced by the mass flow, pipe length and diameter (Rogenhofer, 2018). The design of floor area density and land use distribution directly affects the district's cooling demand distribution and indirectly affects the pipe diameters and mass flow rate. The pipe diameters indicate the capital expenditures on the pipe selection. Finally, in the distribution of chilled water, the thermal loss to be compensated by the additional cooling energy generated by the district cooling plant comes in two ways – the conductive and convective of heat transfer (Keçebaş et al., 2011). The temperature gap between the chilled water and the soil leads to the former and the pipe diameter affects the latter (Bergman et al., 2017). For the existing studies, Chow et al. optimized the land use types for the success of district cooling system implementation in three case studies in Hong Kong (Chow et al., 2004). Best et al. explored the impact of various combinations of land use on the performance of the district energy supply system (Best et al., 2015). Using a test case in California, they managed to demonstrate the ratio of certain land use should be restricted for higher performance of the energy supply system. However, the studies above including those focusing on peak-shaving or valley-filling did not consider the potential impact of the spatial distributions of the land use.

Figure 3 summarizes the links between the design of floor area density and land use distribution and the affected DCS expenditures. The affected capital expenditures include that spent on the piping, chiller & cooling towers, and pumps (denoted as $CAPEX_{piping}$, $CAPEX_{CH\&CT}$, and $CAPEX_{pump}$). The affected operational expenditures include that spent on the thermal loss, pressure drop, and cooling demand (denoted as $OPEX_{qloss}$, $OPEX_{\Delta p}$, and $OPEX_{\mathrm{qc}}$). In this work, the five indicators of DCS cost-effectiveness are the annualized $CAPEX_{piping}$, $CAPEX_{CH\&CT}$, and $CAPEX_{pump}$ together with the annual $OPEX_{qloss}$ and $OPEX_{\Delta p}$ divided by the district's annual cooling demand. Denoted as $aCAPEX_{piping}$, $aCAPEX_{CH\&CT}$, $aCAPEX_{pump}$, $aOPEX_{qloss}$, and $aOPEX_{\Delta p}$, their calculations can be found in Section 2.4.3.

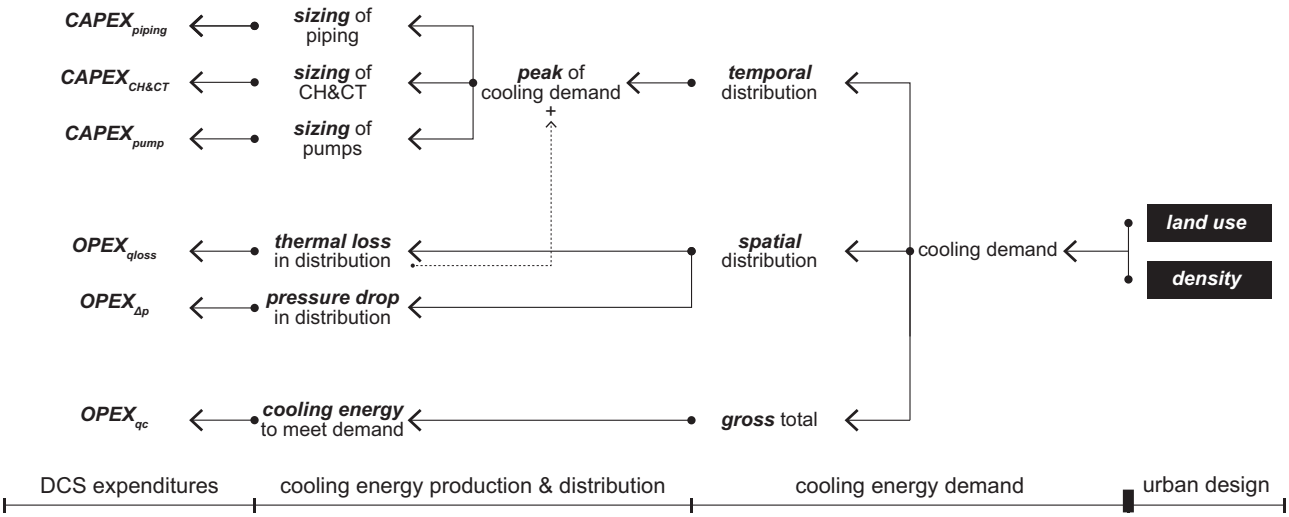

Figure 3. Links between urban density, land use, and the cost-effectiveness of DCS components.

Sensitivity analysis identifies and some quantify the importance of the input variables to the output variability (Mavromatidis et al., 2018). It has been widely used in studies on building design and building energy performance (Tian, 2013). Three methods of sensitivity analysis have been commonly used on investigations in building energy performance through simulations (Kristensen & Petersen, 2016). They are local sensitivity analysis, Morris Method, and Sobol' method. Without giving out the actual ranking of the input variables, local sensitivity analysis identifies a group of the more sensible ones (Kristensen & Petersen, 2016). The latter two gives out the ranking, while the Sobol' method even quantifies the importance. The effect indices comes in two orders: the first-order effects and the second-order effects. The former quantifies the impacts of the input variables independently, while the latter also considers the interactions between the input variables (Petersen et al., 2019). Methods to balance the main disadvantage of the Sobol' method, high computational cost, are as follows. One can adopt an efficient quasi-Monte Carlo sampling technique; simulate a small number of samples and apply a predictive model to amplify simulated dataset; or use fast simulation tools (Shmueli et al., 2017; Tian, 2013).

The CEA simulations are performed on hourly-basis over a year of 8,760 hours. With a connection to a parametric geometric urban design model in Grasshopper (Shi, 2019), CEA is able to automate iterations of energy simulations for the sensitivity analysis. Examples of similar energy simulation tools include the Ladybug and Honeybee (Roudsari & Pak, 2013) Grasshopper plugins and the Urban Modeling Interface (UMI) (Reinhart et al., 2013). Both tools can forecast the cooling demand for a given scenario of urban design. However, neither of them is able to design the DCS piping network or calculate the thermal loss and pressure drop in the process of cooling energy distribution.

This study targets at providing urban designers with insights on how to spatially distribute floor area density and land use for the DCS cost-effectiveness. These insights can be used at the early stages of urban design for a tropical high-density district serviced by district cooling systems (DCS). We aim to answer the following two research questions, taking Singapore as an example. (1) To what extent do the distributions of density (floor area ratio) and land use influence the cost-effectiveness of a DCS? (2) How to spatially distribute the urban density and land use for a cost-effective DCS, at the early stage of urban design processes?

Nomenclature

DCS	district cooling system
$CAPEX$	capital expenditure [USD]
$OPEX$	operational expenditure [USD]
$aCAPEX$	annualized capital expenditure cost-effectiveness [USD/MWh]
$aOPEX$	annual operational expenditure cost-effectiveness [USD/MWh]
CEA	City Energy Analyst

2. Methods

The methodological framework of this research had a five-step workflow (Figure 4). The first four steps are detailed in this section. The fifth step is presented in Section 3. Section 2.1 describes the sources of data used in this study. Section 2.2 describes the input variables of our experiments after preprocessing. Section 2.3 describes the methods used for the experimental design. Finally, Section 2.4 describes the tools used to assess the performance of the DCS cost-effectiveness.

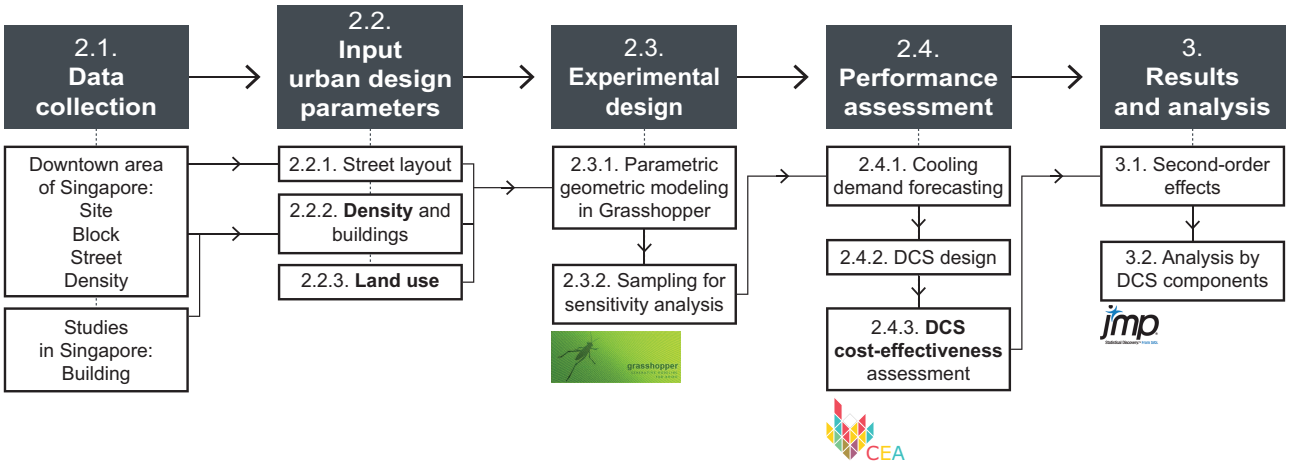

Figure 4. The five-step workflow and the tools used in this study.

2.1. Data collection

We gathered the GIS data about the street layout and the floor area ratio for each block of Downtown Singapore (Figure 5). These data were retrieved from the Singapore Master Plan 2014 (Urban Redevelopment Authority, 2014). We took this information as the reference to set the input parameters and boundaries of design variables. By doing so, we limit the variations of urban density and land use distributions within the development framework envisioned by the local planning authority. This framework included the street layout connections to the surroundings and the restrictions on the floor area development. In addition, in the Master Plan, there was little data available concerning the building footprints in the blocks, since this area was planned yet with few occupying buildings. Such data included the shape of the building

footprints and their site coverage, which were necessary as input urban design parameters. We referred to and extracted data from the relevant existing studies in Singapore for the missing data and details are explained in Section 2.2.2 (Shi et al., 2019).

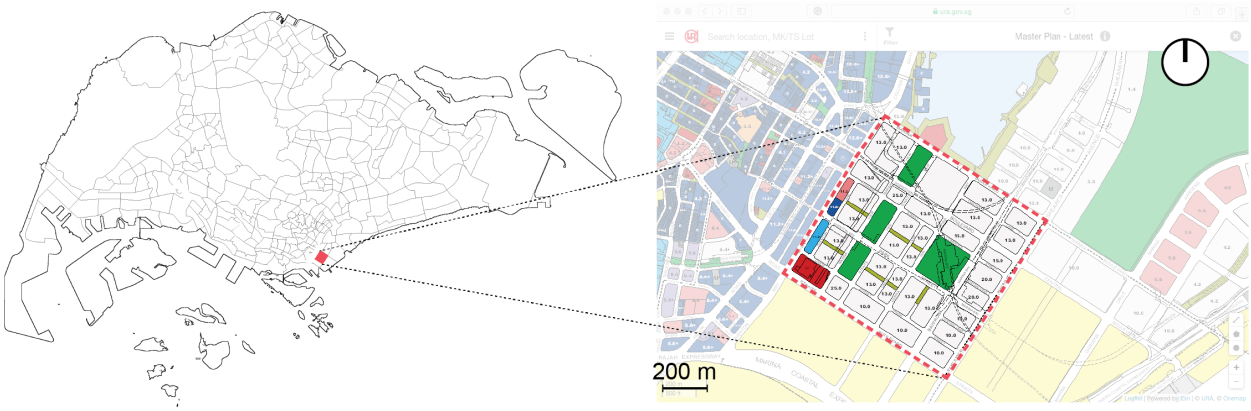

Figure 5. The location of the case study at Downtown Singapore and the Singapore Master Plan 2014

2.2. Input urban design parameters

This subsection serves to introduce the input variables and parameters that build up the parametric geometric model for the sampling of sensitivity analysis. Besides those related to density (Section 2.2.2) and land use (Section 2.2.3), for the design of district cooling systems, those regarding the street layout were also required (Section 2.2.1).

2.2.1. Street layout

We used the data of Section 2.1 to extract all street segments (in-between intersections) of Downtown Singapore. For each street segment, we extracted the information about their length and width. This information was important for the DCS design for two reasons provided the piping network usually follows the street layout. The first was that it affected the length and diameter of the piping network. The second reason was that it affected the cooling energy demand of each end-user by providing the space in-between buildings for mutual shading and solar radiation.

2.2.2. Density and buildings

We used Density gradient to measure the spatial distribution of density (floor area ratio). In this study, Density gradient (ranging from - ∞ to ∞) described the proximity of high or low floor area ratio to the DCS cooling plant. When all the blocks serviced by the DCS cooling plant had the same floor area ratio, the Density gradient was zero. When the blocks closer to and further away from the DCS cooling plant had a higher floor area ratio, the Density gradient was respectively above and below zero. The more the Density gradient was away from zero, the more the difference in floor area ratio among the blocks was. The concept of the Density gradient is furthermore illustrated in Figure 6.

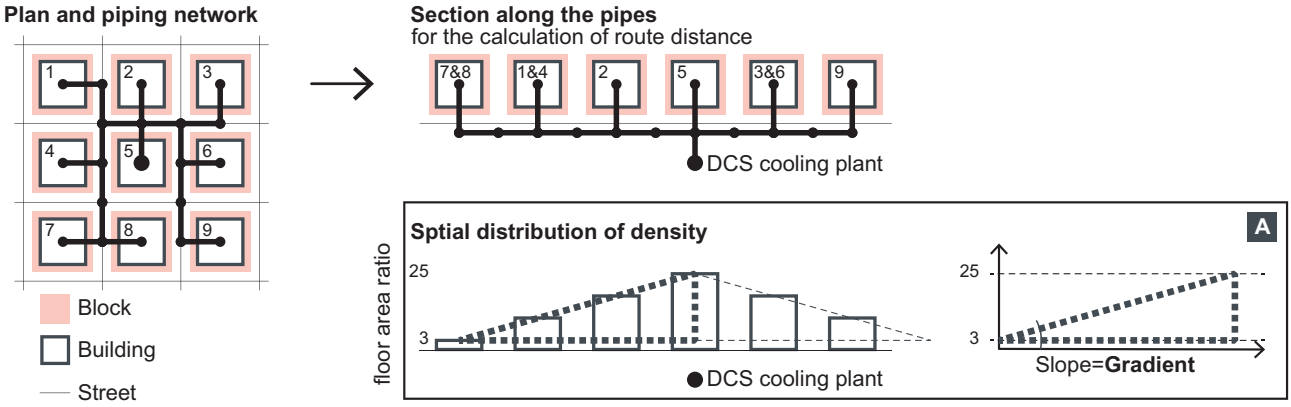

Figure 6. Route distance between buildings and the DCS cooling plant, Density gradient, and their calculations (A).

As illustrated in Figure 6, the Density gradient equaled the difference in floor area ratio between the furthest and the closet block to the DCS cooling plant divided by the route distance between these two blocks. The route distance between two nodes on a piping network measured the total length of all pipe segments connecting these two nodes. The range of floor area ratio for each block was kept between 3 and 25, based on the minimum requirement for a block to be qualified as high-density and the highest floor area ratio found in the Singapore Master. The longest route distance found in the Downtown Singapore between the DCS cooling plant located at the centroid of the district and the furthest block was approximately 1,010 m. In consequence, the lower and upper limits of the Density gradient were respectively set between ± (25-3)/1010 = ± 0.02718 m^{-1}. The gross floor area of this district envisioned by the local planning authority was approximately 5,000,000 sqm. This number of floor area remained constant for all samples to be generated throughout this study. The floor area ratio of each block could be calculated based on both the district's gross floor area and the Density gradient.

2.2.3.Land use

Three land use - residential, office, and retail – were used in this study as they are the most dominant land use in the Master Plan of Singapore (Urban Redevelopment Authority, 2014). Two variables, Residential gradient, and Office gradient were respectively used to measure the distribution of the land use of residential and office. As illustrated in Figure 7, land use gradients were calculated with a similar method as that of Density gradient. Instead of floor area ratio, in calculating land use gradient, we used land use ratio. The lower and upper limits of land use ratios were between 0 and 1. Thus, the lower and upper limits of the two land use gradients were between ± (1-0)/1010 = ± 0.00099 m^{-1}. Two more input variables, Initial residential ratio and Initial office ratio, were needed as the input variables for the sensitivity analysis. As the initial states of either Residential gradient or Office gradient, they were the corresponding land use ratios of the blocks furthest from the DCS cooling plant. These four input variables together helped to calculate the share of the floor area of residential and office in a block over the block's gross floor area. When the sum of these two land use ratio was larger than 1, both of them were proportionally reduced as illustrated in Figure 7 until the sum equaled 1. The land use ratio of retail of each block was calculated as 1 subtracted by the sum of the land use ratio of residential and office. Additionally, the share of the floor area of a particular land use type in the entire district over the district's gross floor area was named as Global land use ratio. Table 1 summarizes the major urban design parameters mentioned above and the five independent input variables are indicated.

Table 1. A summary of the major urban design parameters involved.

Urban design parameters	Input variables	Boundary	Definition
Floor area ratio [-]	-	[2, 25]	Ratio of gross floor area in a block/district to the site area of that block/district
Density gradient [m^{-1}]	Yes	[± 0.02718]	
Land use ratio [-]	-	[0, 1]	Ratio between the floor area of each land use type in a block
Route distance [m]	-	[0, 1010]	The total length of all pipe segments connecting two nodes
Residential gradient [m^{-1}]	Yes	[± 0.00099]	The residential land use ratio of the block closest to the district cooling plant minus the equivalent of the block furthest from the district cooling plant, then divided by the route distance between the two blocks
Office gradient [m^{-1}]	Yes	[± 0.00099]	Same as above
Global land use ratio [-]	-	sum = 1	Ratio between the gross floor area of each land use type in the district
Initial residential ratio [-]	Yes	[0, 1]	The residential land use ratio of the block furthest from the district cooling plant
Initial office ratio [-]	Yes	[0, 1]	Same as above

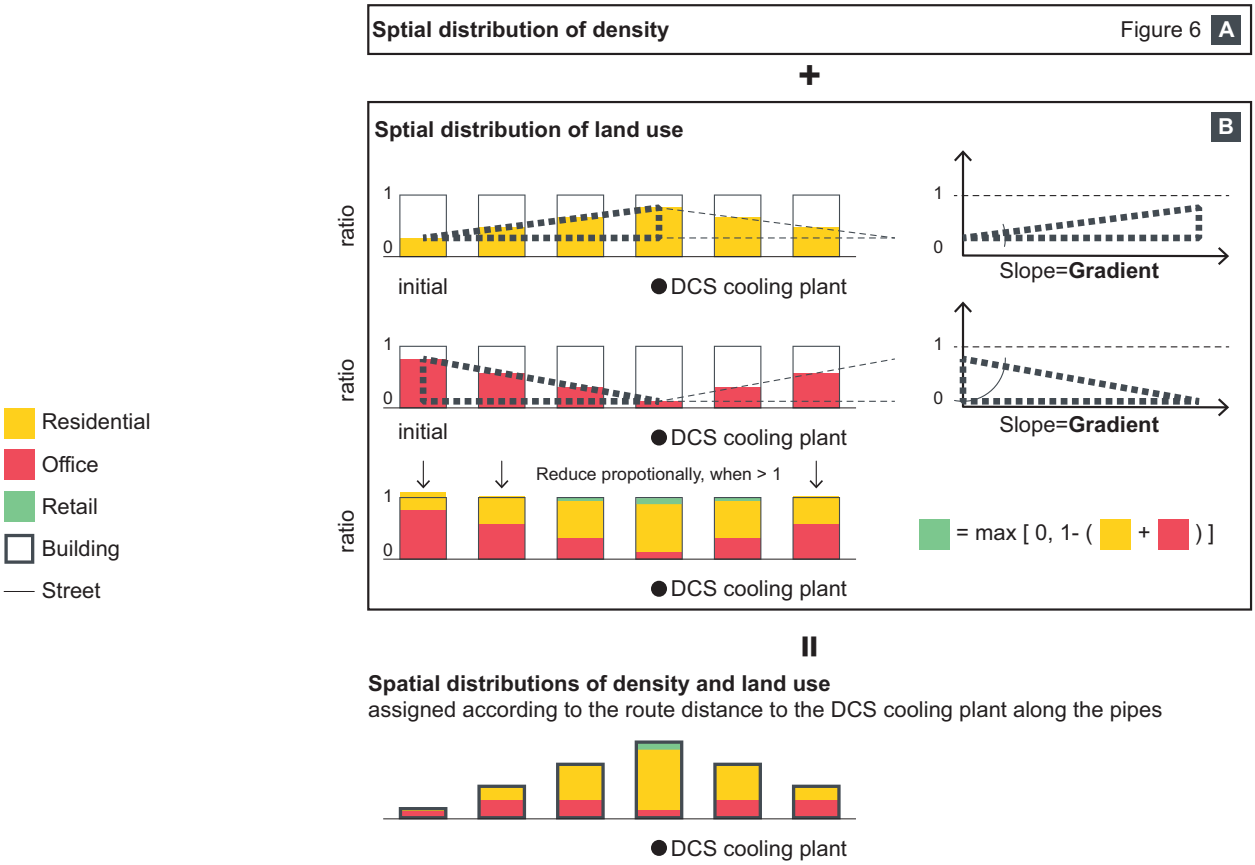

Figure 7. Residential and office land use gradient, the ratio of retails, and their calculations; Density and land use ratios assigned to each block/building. The A for Urban density distribution stands for the A that can be found in **Figure 6**.

2.3. Experimental design

2.3.1.Parametric geometric modeling in Grasshopper

Based on the input parameters and the five independent variables explained in the previous section, we built the parametric geometric model of the district serviced by a DCS in the Grasshopper tool. The model coupled (Shi, 2019) with the City Energy Analyst (CEA) allowed the iteration of urban form generation, energy simulations, and performance assessment for the sensitivity analysis. Figure 8 provides two examples of districts generated by this parametric geometric model built in Grasshopper. The one on the left side (Figure 8a) has a Density gradient of 0.02046, a Residential gradient of -0.00040, an Office gradient of -0.00049, a Global ratio of the three land use of 0.77 : 0.20 : 0.03 (residential : office : commercial). The one on the right side (Figure 8b) has a Density gradient of -0.02174, a Residential gradient of -0.00059, an Office gradient of -0.00043, and a Global ratio of the three land use of 0.13 : 0.76 : 0.11 (residential : office : commercial). Both examples have a gross floor area of 5,000,000 sqm. Both examples show how floor area ratio and land use ratio of each block were manipulated by the five design input variables and the district's gross floor area restriction.

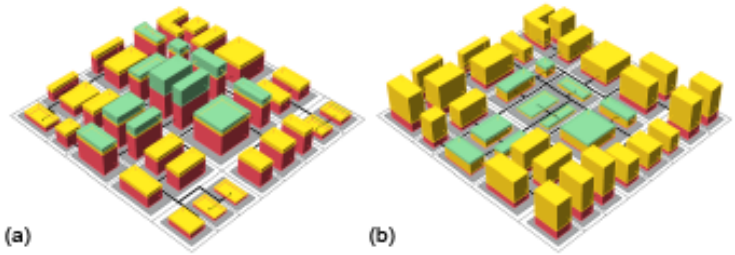

Figure 8. Two examples of districts generated by the parametric geometric model in Grasshopper.

2.3.2. Sampling for the sensitivity analysis

To complete a full performance assessment of one sample, it may take from four to six hours. To apply Sobol' method sensitivity analysis and overcome its heavy computational expenses, we used the quasi-Monte Carlo sampler (Saltelli et al., 2010) using SALib (Herman & Usher, 2017) and an artificial neural network to amplify the number of the simulated samples with JMP Pro 13 (SAS Institue Inc., 2016). For the sampling, the sample size was set at $N = 35$ and makes a total number of $N \cdot (2k+2) = 420$ samples, where k equaled 5, the number of input variables. Figure 9 illustrates the probability density function of the sampled values for the five independent input variables defined in Section 2.2.

Artificial neural network has been widely utilized in solving predictive problems for studies on building energy consumptions (Mohandes et al., 2019). It has been used in studies involving various metrics of urban development, though not yet with a focus on the DCS cost-effectiveness (M. Silva et al., 2018). Despite being considered as a "black-box", artificial neural network has demonstrated its great success in terms of the accuracy of predictions (Mohandes et al., 2019; Shmueli et al., 2017; M. C. Silva et al., 2017). Usually, three layers - namely the input layer, the hidden layer, and the output layer - make up an artificial neural network. The relationships between the inputs and the outputs are decided by an activation function. For building energy studies, Linear Function and Hyperbolic Tangent Function are observed as the commonly used activation function (Mohandes et al., 2019). The coefficient of multiple determination (R square) and the mean absolute deviation are the most commonly used measurements for prediction accuracy (Mohandes et al., 2019). The latter describes the average positive difference of the predicted dataset from the simulated dataset. One of the common drawbacks of artificial neural networks is its tendency to overfit the data, and KFold crossvalidation is recommended for a small dataset as in this study (Shmueli et al., 2017). KFold crossvalidation subdivides a dataset into K subsets. Each of the subsets rotates to serve to validate once as the other K-1 subsets serve to train the model of prediction. After a series of rounds of trials for the best R square and mean absolute deviation, the number of neurons, hidden layers, and KFold as well as the activation function were witnessed using the following settings: one hidden layer and 5 neurons with the Hyperbolic Tangent Function; the number of KFold set at 5. The results maight have slight variations from one run to another since the artificial neural network networks were constructed with the technique of Monte Carlo sampling (SAS Institue Inc., 2016).

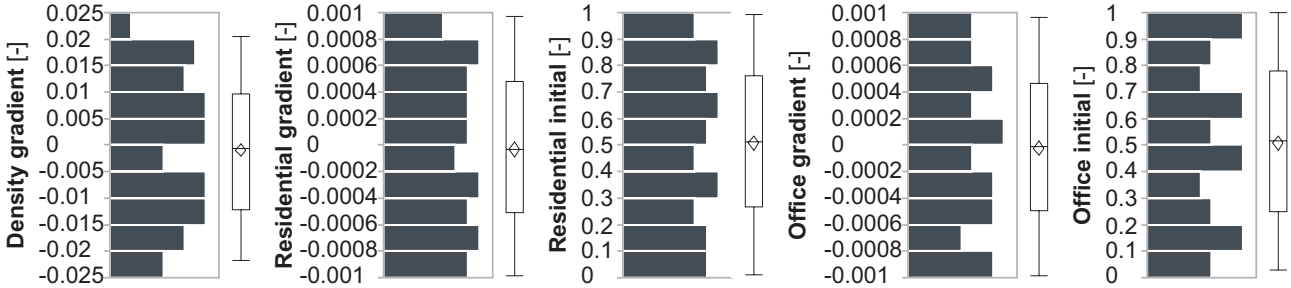

Figure 9. Distribution of the sampled values for the five input variables, Density gradient [-], Residential gradient [-], Initial residential ratio [-], Office gradient [-], and Initial office ratio [-].

2.4. District cooling systems design and assessment

In this paper, for the cooling demand forecasting, district cooling systems design, and the performance assessment, we used the CEA v2.9.2 (The CEA team, 2019).

2.4.1. Cooling demand forecasting

The cooling demand forecasting served to provide the inputs for the DCS design, simulation, and performance assessment. It was conducted for each iteration with the inputs including the building geometries and their spatial locations, as well as the occupancy types (land use), which were from the parametric geometric model in Section 2.3. Other inputs including the ratio of air-conditioned area, the temperature set points, the HVAC technology selection for each DCS component, the properties of the building envelope, the weather conditions in Singapore came from the CEA v2.9.2 Database. The occupancy schedules were adjusted from that of ASHRAE (ASHRAE Project Committee 90.1., 2019). The output of cooling demand forecasting was the hourly cooling demand of each building for every hour over a typical year.

2.4.2. District cooling systems design

Piping network design

In this study, we had the piping network of a DCS follow the street layout, with the connection to each end-user located at the centroid of the building and the cooling plant located in the centroid of the entire district. The piping network design used in all iterations in this study was illustrated as in Figure 10. It had the shortest total length of all pipe segments. A branched layout without loops was used. The network was determined with the Steiner spanning tree algorithm (Cormen et al., 2009) implemented in the CEA v2.9.2 (The CEA team, 2019).

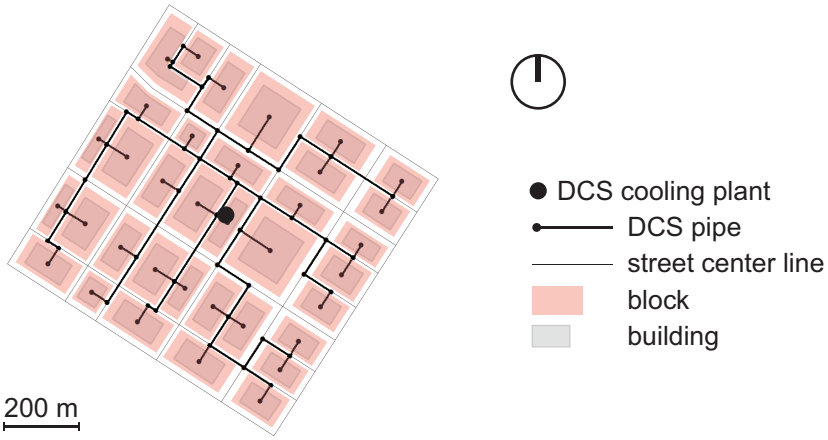

Figure 10. The piping network layout used throughout the simulations in this study.

Cooling energy production and distribution

This step input the results of cooling demand forecasting and the piping network design as well as a series of other parameters (Table 2) concerning the simulations of cooling energy production and distribution. In all 420 iterations, the technology selection for each DCS component was kept the same. The DCS cooling plant contained vapor compression chillers and cooling towers, the sizes of which were decided based on the peak cooling demand and the thermal loss along the network. The pipe width of each segment of the piping network was decided based on the peak mass flow rate. The size of pumps was decided based on the peak pressure drop along the piping network.

Table 2. DCS Input parameters in this study

Parameter	Value	Unit	Note
Thermal conductivity of polyurethane	0.023	W/mK	-
Supply Temperature in DCS networks	~5.4	°C	-
Plant COP	~4.4	-	Including operation of all devices at the cooling plant

2.4.3. Performance assessment

To assess the performance of each of the 420 samples, we used the five indicators of DCS cost-effectiveness. They were the annualized capital expenditures of piping network, cooling plant (chillers and cooling towers), and pumps (denoted as $aCAPEX_{piping}$, $aCAPEX_{CH\&CT}$, and $aCAPEX_{pump}$) as well as the annual operational expenditures of plant and pump (denoted as $aOPEX_{qloss}$, $aOPEX_{\Delta p}$). All the five indicators were normalized to the annual cooling demand, and the unit was USD/MWh. The sum of the five indicators was named the Global DCS expenditure [USD/MWh].

The $CAPEX$ of the pipes, cooling plants, and pumps were based on their required sizes and the technology prices stored in the CEA database. The $aCAPEX$ was calculated from $CAPEX$ using Equation 1, where i stands for the interest rate and n stands for the estimated lifetime (25 years for all technologies, except for 20 years for the cooling towers) as stored in the CEA Database (The CEA team, 2019). $aOPEX_{qloss}$ was the cost of the annual electricity consumed for generating the cooling energy that compensates the thermal loss along the distribution system. $aOPEX_{pump}$ was the cost of the annual electricity consumed for overcoming the pressure drop along the distribution system. The marginal electricity price used in this study was 0.15 USD/KWh (Energy Market Authority, 2018).

$$aCAPEX_{technology} = CAPEX_{technology} \cdot \frac{i(1+i)^n}{(1+i)^n-1} \quad (1)$$

3. Results and analysis

3.1. Second-order effects

Table 3 displays the Second-order effects in the Sobol' SA with the prediction of artificial neural networks in JMP pro 13 and Table 4 shows the two indicators for the performance of the artificial neural network prediction by R square [-] and mean absolute deviation [USD/MWh]. The second-order effects of the five input variables on the five indicators of DCS cost-effectiveness are displayed respectively. Initial residential ratio and Initial office ratio were the first and the second most influential ones. Density gradient was the most important while Residential gradient and Office gradient had much less influence over the DCS cost-effectiveness. The results also showed that the input variables related to the temporal distributions (residential and Initial office ratios) of cooling demand were more dominant than those related to the spatial distributions (Density gradient, Residential gradient, and Office gradient) of cooling demand.

Table 3. The Second-order effects [-] of the five input variables on the five indicators of DCS cost-effectiveness.

	$aCAPEX_{piping}$	$aCAPEX_{CH\&CT}$	$aCAPEX_{pump}$	$aOPEX_{qloss}$	$aOPEX_{\Delta p}$
Density gradient	**0.268**	0.014	**0.443**	0.011	**0.329**
Residential gradient	0.032	0.032	**0.175**	0.028	0.054
Initial residential ratio	**0.699**	**0.7**	0.049	**0.94**	**0.258**
Office gradient	0.005	0.034	0.057	0.002	0.056
Initial office ratio	0.109	**0.345**	**0.377**	**0.124**	**0.258**

Table 4. The performance of the artificial neural network prediction by R square [-] and mean absolute deviation [USD/MWh].

	$aCAPEX_{piping}$	$aCAPEX_{CH\&CT}$	$aCAPEX_{pump}$	$aOPEX_{qloss}$	$aOPEX_{\Delta p}$
R square	0.96	0.89	0.54	0.97	0.85
mean absolute deviation	0.004	0.119	0.013	0.006	0.01

3.2. The cost-effectiveness indicators

Table 5 summarizes the minimum and the maximum values found for the five indicators of DCS cost-effectiveness. The difference between the minimum and the maximum of each indicator ranged from ~ 60% in $aCAPEX_{pump}$ to ~173% in $aOPEX_{qloss}$. As each indicator's contribution to the Global DCS expenditure was dramatically different, the impacts of the temporal and spatial distributions of the cooling demand on the DCS cost-effectiveness shall be analyzed by the DCS components, respectively. Table 6 summarizes the share of the five DCS cost-effectiveness indicators in the Global DCS expenditure combined with that on fulfilling the cooling demand ($aOPEX_{\mathrm{qc}}$) across the 420 samples and Table 7 includes the five indicators only. Except $aOPEX_{\mathrm{qc}}$, $aCAPEX_{CH\&CT}$ was the only DCS cost-effectiveness that has a prominent role out of the five. The rest was close to negligible.

Table 5. The range of normalized $aCAPEX$ and $OPEX$ of the 420 samples by pipe, plant, and pump by annual cooling energy demand in [USD/MWh].

	$aCAPEX_{piping}$	$aCAPEX_{CH\&CT}$	$aCAPEX_{pump}$	$aOPEX_{qloss}$	$aOPEX_{\Delta p}$
min	0.1317	4.486	0.2341	0.0121	0.1599
max	0.231	7.3726	0.3749	0.033	0.4108
(% more than min)	(~75%)	(~72%)	(~60%)	(~173%)	(~157%)

Table 6. The range of the share of the five DCS cost-effectiveness indicators and the expenditure on fulfilling the cooling demand ($OPEX_{\mathrm{qc}}$) out of the total of the six across the 420 samples [-].

	$aCAPEX_{piping}$	$aCAPEX_{CH\&CT}$	$aCAPEX_{pump}$	$aOPEX_{qloss}$	$aOPEX_{\Delta p}$	$aOPEX_{qc}$
min	0.02%	0.52%	0.03%	0%	0.03%	72.51%
max	0.73%	24.73%	1.45%	0.09%	0.78%	99.39%

Table 7. The range of the share of the five DCS cost-effectiveness indicators out of the total of the five across the 420 samples [-].

	$aCAPEX_{piping}$	$aCAPEX_{CH\&CT}$	$aCAPEX_{pump}$	$aOPEX_{qloss}$	$aOPEX_{\Delta p}$	$aOPEX_{qc}$
min	1.94%	83.18%	3.76%	0.16%	2.26%	-
max	4.22%	91.49%	5.63%	0.6%	7.84%	-

3.3. Analysis by district cooling system components

3.3.1. Global DCS expenditure

We used the *k-means* method in JMP pro 13 to produce four clusters of Global land use ratios. Figure 11 plots the performance of the 420 samples in Global DCS expenditure per cluster and per gradient. The Global land use ratio (indicating land use temporal distributions) was more impactful than the Density gradient, Residential gradient, and Office gradient (more indicating the land use spatial distributions). Also, different Global land use ratios might result in similar Global DCS expenditures (the clusters in grey and green). Another observation is that the cluster (red) with a higher Global DCS expenditure had more commercial land use (0.53), while the cluster (yellow) with a lower Global DCS expenditure had more residential land use (0.68).

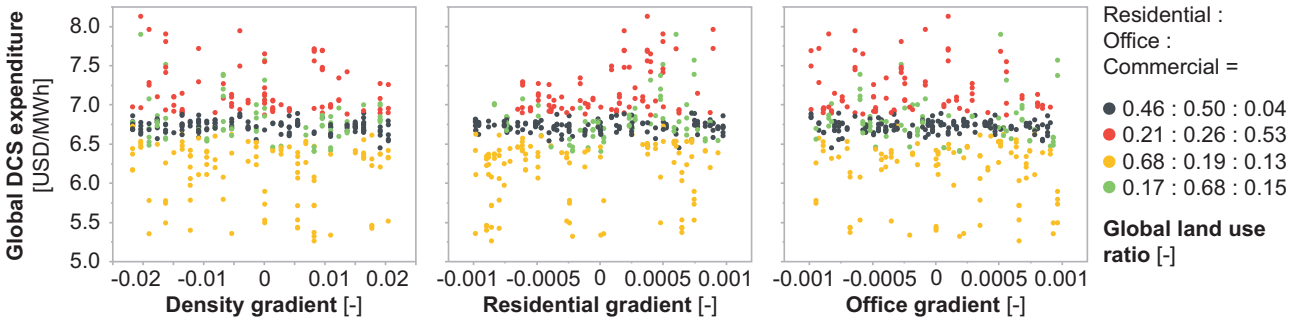

Figure 11. The Global expenditure [USD/MWh] by Density gradient [-], Residential gradient [-], and Office gradient [-], clustered by four groups of Global land use ratios.

3.3.2. Piping network

The sensitivity analysis results showed that both Initial residential ratio and Density gradient had a major influence over $aCAPEX_{piping}$, the annualized capital expenditure of the DCS piping network, accounting for ~2% to ~4% of the Global DCS expenditures. Figure 12 plots the $aCAPEX_{piping}$ of the 420 samples by Global residential ratio and Density gradient. Generally, $aCAPEX_{piping}$ increased as the Global residential ratio increased. For the samples with the same Global residential ratio, $aCAPEX_{piping}$ tent to increase as the Density gradient decreased. Samples with a Global residential ratio under 0.65 and an appropriate Density gradient could possibly bring the $aCAPEX_{piping}$ down by at least 20% compared to the worst-performing one to lower than the mean $aCAPEX_{piping}$ across the 420 samples, as shown in Figure 12.

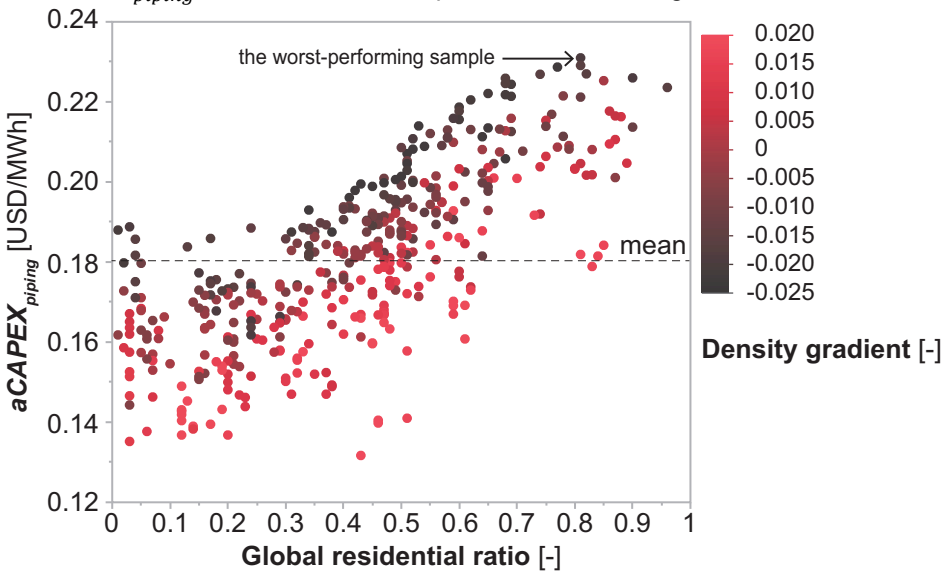

Figure 12. $aCAPEX_{piping}$ [USD/MWh] by overall residential ratio [-] and Density gradient [-].

The diameter of each pipe segment and its pricing affected the $aCAPEX_{piping}$, since the length of each pipe segment remained the same across the 420 samples. Figure 13 (a) shows that the average pipe diameter decreased as the Global residential ratio increased. According to the pricing table of pipes in the CEA database, the unit pipe price did not proportionally decrease with the pipe diameter: the unit price of thinner pipes was higher than that of thicker ones. This explained why the $aCAPEX_{piping}$ increased with the Global residential ratio. Additionally, Figure 13 (a) shows that the average pipe diameter decreased as Density gradient increased for the samples with the same Global residential ratio. Figure 13 (b) shows that samples with the same Global residential ratio have similar annual cooling demand. Higher Density gradient meant more built area and more cooling demand were spatially distributed in proximity to the district cooling plant. Thus, high Density gradient reduced the amount of cooling energy to be distributed to the further side of the piping network and decreased the need for installing thicker pipes resulting at lower $aCAPEX_{piping}$.

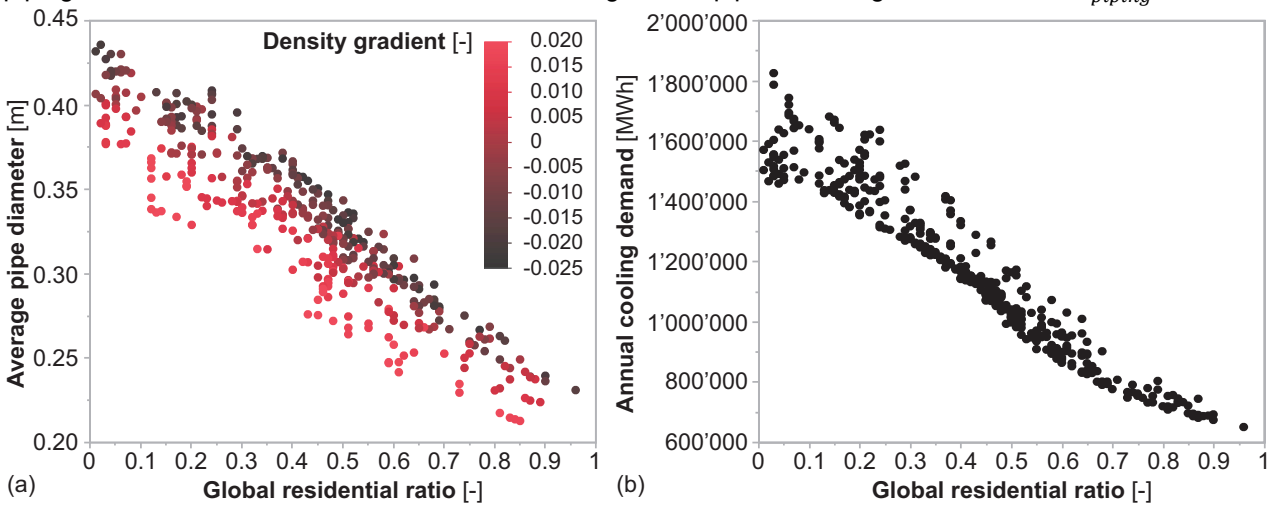

Figure 13. (a) Average pipe diameter [m] by Global residential ratio [-] and Density gradient [-]; (b) Annual cooling demand [MWh] by Global residential ratio [-].

3.3.3. Centralized chiller and cooling tower

The results of sensitivity analysis showed that both Initial residential ratio and Initial office ratio substantially influenced $aCAPEX_{CH\&CT}$, the annualized capital expenditure of the centralized chiller and cooling tower. It accounted for as much as ~83% to ~91% of the Global DCS expenditures. Figure 14 (a) plots the $aCAPEX_{CH\&CT}$ of the 420 samples by their Global residential ratio and Global office ratio. Generally, $aCAPEX_{CH\&CT}$ decreased at various rates as the Global residential ratio increased. The decrease rate almost plateaued when the Global residential ratio was between ~0.25 and ~0.5. Samples with a Global residential ratio at this range could possibly bring the $aCAPEX_{CH\&CT}$ down by ~15% to ~25% compared to the worst-performing one. This plateau meant more flexibility for various combinations of Global land use ratios. A much higher Global residential ratio significantly reduced the $aCAPEX_{piping}$ yet undermined the possibilities for mixed-use design. Additionally, for the samples with the same Global residential ratio, $aCAPEX_{CH\&CT}$ tent to increase with the Global office ratio.

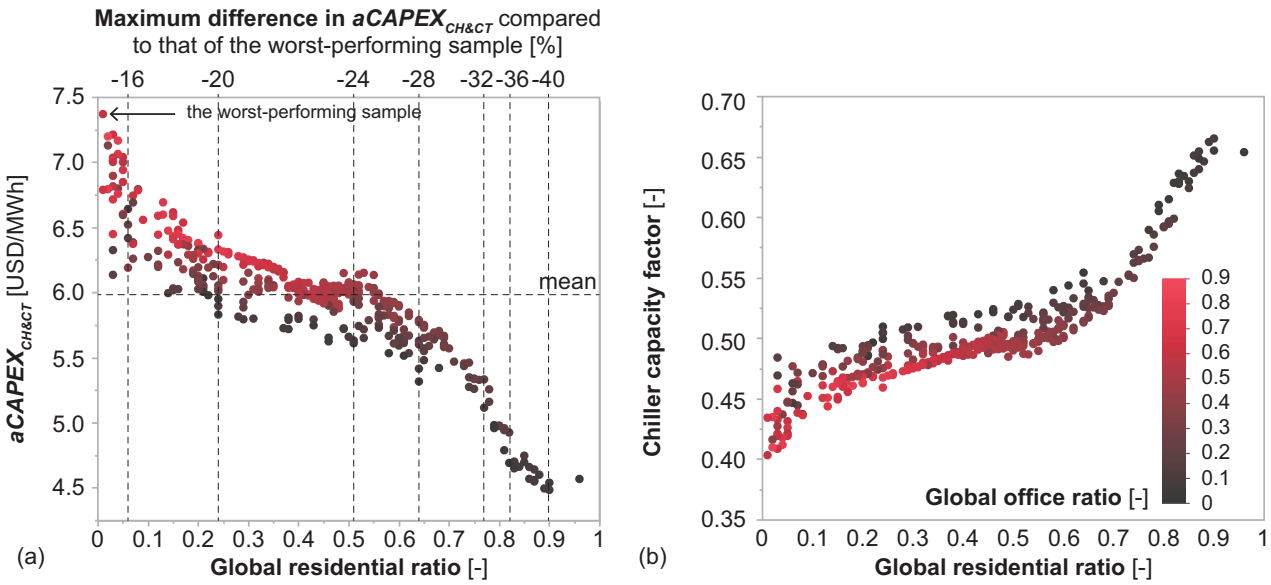

Figure 14. $aCAPEX_{CH\&CT}$ [USD/MWh] by Global residential ratio [-] and Global office ratio [-].

The $aCAPEX_{CH\&CT}$ depended on the usage or the capacity factor of the centralized chiller and cooling tower. The capacity factor was calculated as the ratio of actual cooling energy generated divided by the maximum cooling energy generated if the system continuously functioned at its nominal capacity over the same period of time (see Equation 2). We calculated the capacity factor for the DCS chillers (CH). It generally increased as the Global residential ratio increased while the Global office ratio decreased in Figure 14 (b). This was due to certain land use combinations (e.g., higher Global residential ratio, lower Global office ratio) helped to shave the peak or fill the valley of cooling demand, which affected the nominal capacity design of a DCS cooling plant.

$$Capacity\ factor_{chiller} = \frac{Annual\ cooling\ energy\ generated}{365\ days \cdot 24\ hours/day\ \cdot\ Nominal\ capacity} \quad (2)$$

Besides, the sensitivity analysis results showed that both Initial residential ratio and Initial office ratio had a major influence on the annual DCS operational expenditure on compensating the thermal loss in distributing the cooling energy ($aOPEX_{qloss}$). Figure 15 plots the $aOPEX_{qloss}$ of the 420 samples by their Global residential ratio and Global office ratio. $aOPEX_{qloss}$ increased as the Global residential ratio and Global office ratio increased. Keeping the Global residential ratio under ~0.5 can reduce the $aOPEX_{qloss}$ by ~30%. This was because higher Global residential ratio came with thinner pipes (See Figure 13 (a)), and thinner pipes had more thermal loss. This was due to that the proportional insulation thickness (and hence thermal resistance) of thinner pipes was lower per every unit of mass flow, in comparison to thicker pipes. However, $aOPEX_{qloss}$ was almost negligible, as the temperature difference between the chilled water and the soil was relatively small and this indicator merely accounted for less than 1% of the Global DCS expenditures.

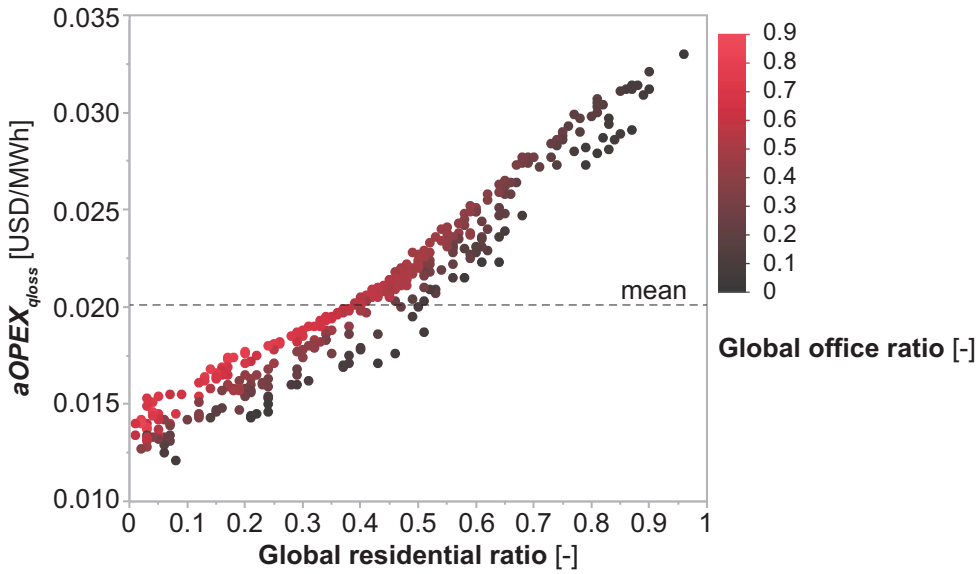

Figure 15. $\boldsymbol{aOPEX_{qloss}}$ [USD/MWh] by Global residential ratio [-] and Global office ratio [-].

3.3.4. Pumps

The sensitivity analysis results showed that Density gradient, Initial office ratio, and Residential gradient have a major influence over $aCAPEX_{pump}$, the annualized capital expenditure of the DCS pumps. However, no obvious trend was witnessed for the $aCAPEX_{pump}$ by any of the input variables and it merely accounted for ~ 4% to ~6% of the Global DCS expenditures. For the annual operational expenditure of DCS pumps, denoted as $aOPEX_{\Delta p}$, the sensitivity analysis results showed that Initial office ratio, Initial residential ratio, and Density gradient were of substantial importance. Figure 16 plots the $aOPEX_{\Delta p}$ of the 420 samples by Global office ratio, Global residential ratio, and Density gradient. Samples with a Global residential ratio under ~0.75 or a Global office ratio above ~0.1 could possibly bring the $aaOPEX_{\Delta p}$ down by at least ~50% compared to the worst-performing one. For these samples with the same Global residential ratio or Global office ratio, $aOPEX_{\Delta p}$ tent to decrease by up to ~50% as the Density gradient increased (more built area in proximity to the DCS cooling plant). However, similar to $aCAPEX_{pump}$, $aOPEX_{\Delta p}$ merely accounted for ~2% to ~8% of the Global DCS expenditures.

The behavior of $aOPEX_{\Delta p}$ can be explained in two ways. One is that, of the 420 samples, those more dominated by residential uses had thinner pipes and more extended periods of high mass flow rate, which both caused a higher pressure drop in the process of distributing the cooling energy. The other way is that for samples with the same/similar Global land use ratios and cooling demand, those with more end-users further away (lower Density gradient) from the DCS cooling plant tent to have more pressure drops.

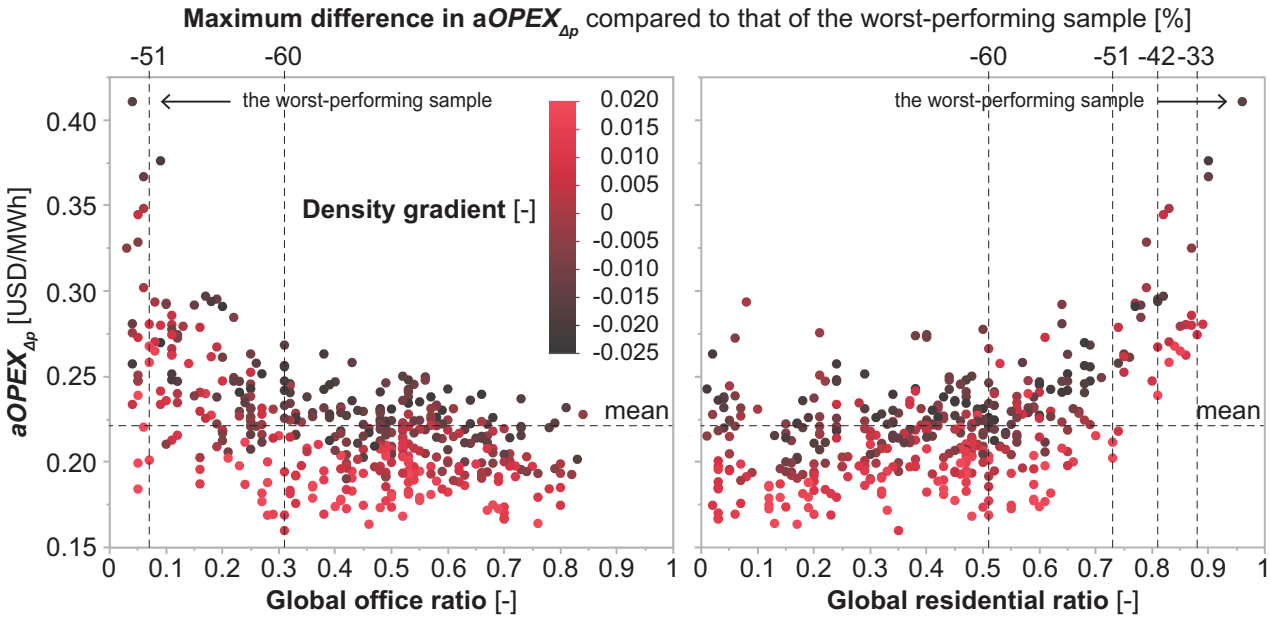

Figure 16. $aOPEX_{\Delta p}$ [USD/MWh] by Global residential ratio [-] and Density gradient [-].

4. Discussion

4.1. Global residential land use ratio

Three observations concerning the land use ratios for the DCS cost-effectiveness are summarized as follows. The first observation is that Global land use ratios have a more dominant role than the spatial distribution of density and land use on the DCS cost-effectiveness. This indicates that the Global office ratio shall be reduced to decrease $aCAPEX_{CH\&CT}$ and $aOPEX_{qloss}$, but kept above 0.1 to decrease $aOPEX_{pump}$. In addition, the Global residential ratio shall be kept above 0.25 as high Global residential ratio significantly reduces the $aCAPEX_{CH\&CT}$ and improves the Global DCS cost-effectiveness. In the meantime, to reduce the $aCAPEX_{piping}$, the $aOPEX_{qloss}$, and the $aOPEX_{\Delta p}$ as well as to increase the flexibility for a mixed-use design, the Global residential ratio can be kept below 0.75.

Among the three land use, the residential land use is observed to be of great importance for the DCS cost-effectiveness. For tropical cities that need cooling only, the $aCAPEX_{plant}$ contributes the majority (up to 91% in this study) to the Global DCS cost-effectiveness. It is highly dependent on the capacity factor of the DCS cooling plant, which is the outcome of the combinations of the cooling demand by the end-users of various land use. For the example of Singapore in this study, a higher Global residential ratio increases the capacity factor and the DCS cost-effectiveness. Yet in the range between 0.25 and 0.75 for high-density mixed-use development, a compromise can be established between the DCS cost-effectiveness and the land use design flexibility. However, the result is context-specific, since different human habits, climates, geolocations, air-conditioned areas, and building management consideration can all affect the peak cooling demand and the capacity factor.

An appropriate high residential land use ratio in high-density mixed-use areas helps to achieve urban design goals like proximity to workplaces and all-day vitality in the public space. However, as a matter of fact, in the newly built high-density mixed-use areas, the land use ratios are often quite limited. A recent study on the megaprojects selected eight case studies across countries and cultures: only two of the eight have a Global residential ratio above 0.25 (Christiaanse et al., 2019). The inclusion of residential land use to the high-density areas of the city is subject to the game of multiple stakeholders beyond DCS operators.

Similarly, whether a residential building should be connected to the district cooling system (DCS) or not remains a decision of the residents, the real estate developers, and the service providers. For example, the sellable air-conditioner ledge of the split-units is not subject to the restriction of the gross floor area in Singapore. Thus, it hurts the interests of the real estate developer by connecting the residential building to DCS and removing the sellable air-conditioner ledge (Shi et al., 2017). Even from the perspective of the service provider, residential land use is not always preferred for the lower electricity tariff at night in Singapore. The DCS service provider may produce and store the cooling energy at night and sell it out to

end-users during the peak time, instead of directly fulfilling the cooling demand of the residential buildings at night. In addition, the occupancy schedule of residential land use is often versatile, and it is difficult to predict the residents' behavior. This may affect the peak cooling demand and the system capacity factor, which may affect the DCS cost-effectiveness for the DCS operators.

4.2. Spatial distributions of density and land use

Besides the Global land use ratios, the spatial distribution of density is also comparatively influential to the DCS cost-effectiveness. The Density gradient is observed to be able to affect the $aCAPEX_{piping}$, $aCAPEX_{pump}$, and $aOPEX_{\Delta p}$ for up to 55%. Though these three indicators contribute only 8% to 16% to the Global DCS cost-effectiveness, keeping more built area in proximity to the DCS cooling plant is in line with other urban design strategies as well. For example, transit-oriented development tends to have higher density immediately next to the transit station for higher accessibility and real estate values (Cervero & Guerra, 2011). Moreover, integrating a transit station design with a DCS cooling plant underneath can maximize the usage of the public land and alleviate the conditions of land scarcity in the high-density areas. Also, for example, in Downtown Singapore, the underground pedestrian tunnels connecting the buildings from the transit station may be partially integrated into the Common Service Tunnel Plan. Such integration helps to enhance the advantages of the common service tunnel, such as easy repair and maintenance, and also justify the massive investment in a shorter term.

The role of the spatial distributions of land use on DCS cost-effectiveness though exists, yet is much less critical than that of the density distribution. Among the 420 samples, for those with the same Global land use ratio and density distribution, the impact of land use distribution on DCS cost-effectiveness is witnessed to be less than 2%. This allows high flexibility to the urban designer for assigning the land use ratios for each block without considering its proximity to the DCS cooling plant.

4.3. Limitations

The limitations of this research came in four aspects and shall be addressed in future studies. (1) Regarding the cooling demand forecasting, three points need to be noticed. The first point is that the Podium building pattern used in this research is minimal while in a high-density area, various types of building patterns (e.g. courtyard, slabs, etc.) shall be included for more accurate cooling demand forecasting. The annual peak cooling demand is crucial for the capital expenditure of the centralized chiller and cooling towers, which contribute to the majority of the Global DCS cost-effectiveness. The other point is about the cooling demand simulation tool. For a building consisting of more than one use type (land use), it should be able to conduct the cooling demand forecasting in multiple zones, as different use type may have various ratio air-conditioned area, set-point, etc. As a drawback of CEA simulations in this study, for a mixed-use building, the inputs for the main use type were assigned to the entire building regardless of the characters of the other use types. The last point is that the occupancy schedule of each land use was adopted from the standards of ASHRAE. A more accurate set of occupancy schedules tailored for the Singaporean context should be used in future studies. (2) Regarding the DCS design, all the DCS components are assigned with a given technology. However, other technologies (e.g. pipes with various insulations, seawater-sourced chillers, etc.) shall be included for considerations. (3) Though neural network predictions were used, the sample size for the simulations in the sensitivity analysis is relatively small at 420. However, this is highly dependent on computing complexity. (4) Concerning the various stakeholders in the entire urban design process, we focused on the interests of the DCS operators only, while the perspectives of the real estate developers and the residents also matter. Thus, cooling energy distribution within each block and heat exchangers shall be included in future studies.

5. Conclusions

This paper presented an investigation on the interdependencies between density, land-use, and the cost-effectiveness of district cooling systems in tropical high-density cities. Two research questions were answered as follows, taking Downtown Singapore as an example.

To what extent do the distributions of floor area ratio, as well as the ratios and distributions of land use, influence the DCS cost-effectiveness? From the perspective of DCS operators, the influence of these factors could reach ~60% to ~75% for $aCAPEX$ and ~150% to ~175% for $aOPEX$. The sensitivity analysis showed that the Global land use ratio, especially the Global residential ratio, had the most dominant impact on the Global DCS cost-effectiveness, followed by the spatial distribution of floor area ratio with impacts on the $aCAPEX$ on pipes and pumps as well as the operation expenditure on pumps for up to 55%. The impact of the spatial distributions of land use on the DCS cost-effectiveness exists, yet it is almost negligible as the

operational expenditures on the thermal loss and pressure drop in the cooling energy distribution are minor. Land use design that shaves the peak or fills the valley of the temporal distribution of cooling demand remains the most viable method for improving the DCS cost-effectiveness.

At the early stage of urban design processes, how can the distribution of land use and density help to reach better DCS cost-effectiveness? Based on the analysis and discussion in this research, out of the three types of land use studied, we found that a Global office ratio should be kept above 0.1; Global residential ratio should be kept between 0.25 and 0.75. However, the inclusion of residential buildings to the DCS network is subject to further evaluations, like the interests of other stakeholders or the operating conditions (e.g., the electricity tariff differences between the day and the night). The other one is on the distribution of floor area ratio, though less impactful than the Global land use ratio. A high floor area ratio is advised to be spatially distributed in proximity to the DCS cooling plant along the piping network. By contrast, the spatial distributions of land use have a relatively minor influence on the DCS cost-effectiveness.

Additionally, this paper demonstrated the use of the City Energy Analyst, coupled with a parametric geometric model in Grasshopper. To reduce the time of every iteration, we used the neural network predictions with a commercial tool, the JMP pro, in the Sobol' sensitivity analysis. The outcomes of this research can be used by urban planners and designers in high-density areas of tropical cities serviced by district cooling systems.

Acknowledgments

References

ASHRAE Project Committee 90.1. (2019). *Schedules and internal loads for Appendix C*.

Bergman, T. L., Lavine, A. S., Incropera, F. P., & DeWitt, D. P. (2017). *Fundamentals of Heat and Mass Transfer, 8th Edition*. Wiley & Sons, Inc. https://www.wiley.com/en-us/Fundamentals+of+Heat+and+Mass+Transfer%2C+8th+Edition-p-ES81119320425

Best, R. E., Flager, F., & Lepech, M. D. (2015). Modeling and optimization of building mix and energy supply technology for urban districts. *Applied Energy*, *159*, 161–177. https://doi.org/10.1016/j.apenergy.2015.08.076

Cervero, R., & Guerra, E. (2011). *Urban densities and transit: A multi-dimensional perspective*. UC Berkeley Center for Future Urban Transport. http://www.its.berkeley.edu/sites/default/files/publications/UCB/2011/VWP/UCB-ITS-VWP-2011-6.pdf

Cheng, V., Steemers, K., Montavon, M., & Compagnon, R. (2006). *Urban Form, Density and Solar Potential*. PLEA 2006. https://infoscience.epfl.ch/record/84787?ln=en

Chow, T. T., Chan, A. L. S., & Song, C. L. (2004). Building-mix optimization in district cooling system implementation. *Applied Energy*, *77*(1), 1–13. https://doi.org/10.1016/S0306-2619(03)00102-8

Christiaanse, K., Gasco, A., & Hanakata, N. (2019). *The Grand Projet: Understanding the making and impact of urban megaprojects*. nai010 publishers. https://www.nai010.com/en/publicaties/the-grand-projet/240662#xd_co_f=MmUzN2M2M2VmMWExNzRjZmFkYTE1MzM0OTMzNTg2MDg=~

Cormen, T. H., Leiserson, C. E., Rivest, R. L., & Stein, C. (2009). *Introduction to Algorithms, 3rd Edition* (3rd edition). The MIT Press.

Energy Market Authority. (2018). *EMA : Electricity Tariffs*. https://www.ema.gov.sg/Residential_Electricity_Tariffs.aspx

Fonseca, J. A., Nguyen, T.-A., Schlueter, A., & Marechal, F. (2016). City Energy Analyst (CEA): Integrated framework for analysis and optimization of building energy systems in neighborhoods and city districts. *Energy and Buildings*, *113*, 202–226. https://doi.org/10.1016/j.enbuild.2015.11.055

Guelpa, E., Toro, C., Sciacovelli, A., Melli, R., Sciubba, E., & Verda, V. (2016). Optimal operation of large district heating networks through fast fluid-dynamic simulation. *Energy*, *102*, 586–595. https://doi.org/10.1016/j.energy.2016.02.058

Herman, J., & Usher, W. (2017). SALib: An open-source Python library for Sensitivity Analysis. *Journal of Open Source Software*, *2*(9). https://doi.org/10.21105/joss.00097

Keçebaş, A., Ali Alkan, M., & Bayhan, M. (2011). Thermo-economic analysis of pipe insulation for district heating piping systems. *Applied Thermal Engineering*, *31*(17), 3929–3937. https://doi.org/10.1016/j.applthermaleng.2011.07.042

Kristensen, M. H., & Petersen, S. (2016). Choosing the appropriate sensitivity analysis method for building energy model-based investigations. *Energy and Buildings*, *130*, 166–176. https://doi.org/10.1016/j.enbuild.2016.08.038

Li, Y., Rezgui, Y., & Zhu, H. (2017). District heating and cooling optimization and enhancement – Towards integration of renewables, storage and smart grid. *Renewable and Sustainable Energy Reviews*, *72*(Supplement C), 281–294. https://doi.org/10.1016/j.rser.2017.01.061

Mavromatidis, G., Orehounig, K., & Carmeliet, J. (2018). Uncertainty and global sensitivity analysis for the optimal design of distributed energy systems. *Applied Energy*, *214*, 219–238. https://doi.org/10.1016/j.apenergy.2018.01.062

McCabe, R. E., Bender, J. J., & Potter, K. R. (1995). Subsurface ground temperature: Implications for a district cooling system. *ASHRAE Journal*, *37*(12). https://www.osti.gov/biblio/215474

Mohandes, S. R., Zhang, X., & Mahdiyar, A. (2019). A comprehensive review on the application of artificial neural networks in building energy analysis. *Neurocomputing*, *340*, 55–75. https://doi.org/10.1016/j.neucom.2019.02.040

Petersen, S., Kristensen, M. H., & Knudsen, M. D. (2019). Prerequisites for reliable sensitivity analysis of a high fidelity building energy model. *Energy and Buildings*, *183*, 1–16. https://doi.org/10.1016/j.enbuild.2018.10.035

Reinhart, C. F., Dogan, T., Jakubiec, J. A., Rakha, T., & Sang, A. (2013). UMI - An urban simulation environment for building energy use, daylighting and walkability. *Proceedings of BS 2013: 13th Conference of the International Building Performance Simulation Association*, *476–483*.

Rogenhofer, L. (2018). *Thermal and hydraulic modelling and optimization of thermal networks in districts in the CEA framework*. https://www.research-collection.ethz.ch/handle/20.500.11850/310828

Roudsari, M. S., & Pak, M. (2013). *Ladybug: A parametric environmental plugin for Grasshopper to help designers create an environmentally-conscious design*. 13th Conference of International Building Performance Simulation Association, Chambery, France.

Saltelli, A., Annoni, P., Azzini, I., Campolongo, F., Ratto, M., & Tarantola, S. (2010). Variance based sensitivity analysis of model output. Design and estimator for the total sensitivity index. *Computer Physics Communications*, *181*(2), 259–270. https://doi.org/10.1016/j.cpc.2009.09.018

SAS Institue Inc. (2016). *JMP 13* (Version 13) [Computer software].

Shi, Z. (2019). Grasshopper-to-CEA Part 2: Running CEA commands in Grasshopper. *City Energy Analyst (CEA)*. https://cityenergyanalyst.com/blog/2019/5/17/grasshopper-to-cea-part-2-creating-input-files-in-shp-format

Shi, Z., Fonseca, J. A., & Schlueter, A. (2017). *Building regulations and urban policies as incentives for application of district cooling systems in Singapore*. World Sustainable Built Environment Conference 2017 Hong Kong, Hong Kong.

Shi, Z., Fonseca, J. A., & Schlueter, A. (2019). *Estimating the renewable energy potential with block typologies*.

Shmueli, G., Bruce, P. C., Stephens, M. L., & Patel, N. R. (2017). *Data Mining for Business Analytics: Concepts, Techniques, and Applications with JMP Pro*. John Wiley & Sons Inc. https://www.wiley.com/en-sg/Data+Mining+for+Business+Analytics%3A+Concepts%2C+Techniques%2C+and+Applications+with+JMP+Pro-p-9781118877432

Silva, M. C., Horta, I. M., Leal, V., & Oliveira, V. (2017). A spatially-explicit methodological framework based on neural networks to assess the effect of urban form on energy demand. *Applied Energy*, *202*, 386–398. https://doi.org/10.1016/j.apenergy.2017.05.113

Silva, M., Leal, V., Oliveira, V., & Horta, I. M. (2018). A scenario-based approach for assessing the energy performance of urban development pathways. *Sustainable Cities and Society*, *40*, 372–382. https://doi.org/10.1016/j.scs.2018.01.028

The CEA team. (2019). *City Energy Analyst v2.9.2*. Zenodo. https://doi.org/10.5281/zenodo.1487867

Tian, W. (2013). A review of sensitivity analysis methods in building energy analysis. *Renewable and Sustainable Energy Reviews*, *20*, 411–419. https://doi.org/10.1016/j.rser.2012.12.014

UNEP. (2015). *District energy in cities: Unlocking the potential of energy efficiency and renewable energy*.

Urban Redevelopment Authority. (2014). *Master Plan*. https://www.ura.gov.sg/uol/master-plan.aspx?p1=view-master-plan#